Vol 15 No 7, July 2006
1009-1963/2006/15(07)/1631-07

Chinese Physics

© 2006 Chin. Phys. Soc.
and IOP Publishing Ltd

Absolute stability of the solidification interface in a laser resolidified Zn–2wt.%Cu hypoperitectic alloy*

Su Yun-Peng(苏云鹏), Lin Xin(林 鑫),
Wang Meng(王 猛), Xue Lei(薛 蕾), and Huang Wei-Dong(黄卫东)

State Key Laboratory of Solidification Processing,
Northwestern Polytechnical University, Xi'an 710072, *China*

(Received 11 October 2005; revised manuscript received 7 December 2005)

This paper reports on laser surface remelting experiments performed on a Zn–2wt.%Cu hypoperitectic alloy by employing a 5kW CW CO_2 laser at scanning velocities between 6 and 1207mm/s. The growth velocities of the microstructures in the laser molten pool were accurately measured. The planar interface structure caused by the high velocity absolute stability was achieved at a growth velocity of 210 mm/s. An implicit expression of the critical solidification velocity for the cellular–planar transition was carried out by nonlinear stability analyses of the planar interface. The results showed a better agreement with the measured critical velocity than that predicted by M–S theory. Cell-free structures were observed throughout the whole molten pool at a scanning velocity of 652 mm/s and the calculated minimum temperature gradient in this molten pool was very close to the critical temperature gradient for high gradient absolute stability (HGAS) of the η phase. This indicates that HGAS was successfully achieved in the present experiments.

Keywords: rapid solidification, absolute stability, laser surface resolidification, Zn–Cu peritectic alloy
PACC: 8130F, 4262A, 8100

1. Introduction

The morphologic instability of a growing solid/liquid interface is the origination of all solidification pattern evolution. Experimental and theoretical studies on solidification morphologic instability have been performed in the last several decades. In the 1960s, Mullins and Sekerka firstly performed the rigorous linear kinetic stability analysis on the planar liquid–solid interface for a dilute binary system and low Peclet number.[1,2] With their efforts, the famous M–S theory was presented in 1964, which predicted the probability of the high velocity absolute stability (HVAS). Since then, some important advances have been made in fundamental understanding of interface morphologic stability: a more complete stability analysis was proposed and extended for large Peclet numbers by Trivedi and Kurz,[3] nonlinear stability analyses were carried out by Wollkind and Segel,[4] Langer and Turski [5,6] and the others[7,8] and nonsteady state interface stabilities were researched by Warren and Langer[9] and Lin *et al.*[10,11] In 1997, a further analysis of the M–S stability criterion which was performed by Ding *et al* predicted a new phenomenon, the high gradient absolute stability (HGAS). It means that when the temperature gradient exceeds a critical value, the solidification interface becomes absolutely stable no matter how large the solidification velocity is.[12]

Although major progress on microstructure evolution has been made, both theoretical and experimental researches have been focused on the HVAS of single phase alloy.[13−16] Until now, there have been few experimental investigations on HVAS of multi-phase alloy and the HGAS. With the development of laser surface remelting technology, it is possible to experimentally achieve above processes on peritectic alloy to investigate the interface stability of a peritectic system, which is favoured for providing experimental foundation for the establishment of precise and quantitative solidification theory of the aforementioned system.

During laser surface remelting, there is an extremely high temperature gradient ($> 10^6$ K/m) in the melting pool and the local growth rate can also reach

*Project supported by the National Natural Science Foundation of China (Grant Nos 50201012 and 50471065).

a very high value (> 1 m/s). Furthermore, one could obtain unidirectional growth structures by adjusting processing parameters. In the melting pool, the local growth rate can be determined directly by $v_s = v_b \cos\theta$, where θ is the angle between the laser beam scanning velocity v_b and the local interface growth velocity v_s,[17] and the local temperature gradient can be determined by numerical calculations.[18] So it is possible to compare the experimental results with the theoretical predictions of the HVAS and HGAS.

This paper reports on laser surface remelting experiments performed to investigate the interface stability under ultra-high temperature gradient and growth velocity of a hypoperitectic Zn–2 wt.%Cu alloy. This alloy was selected due to its narrow solidification temperature interval and its rather complete and credible thermophysical parameters. In this paper, the angle θ was measured by a sampling method similar to the one adopted by Pan *et al.*[19]

2. Experimental details

Zn–2 wt.% Cu alloy was prepared by electric resistance melting of the 99.995% Zn and 99.999% Cu in high pure corundum crucible under high pure argon atmosphere and then poured into a 14 mm×14 mm×90 mm rectangular steel mould with chalk powder coating. In order to remove the oxide of metal on the surface, the outer 1 mm of the ingot was milled off. Specimens of 6 mm×12 mm×30 mm were cut from the remaining ingot. All the specimens were polished up to 500 grid SiC paper and thoroughly cleaned in acetone to obtain a similar surface quality for each one.

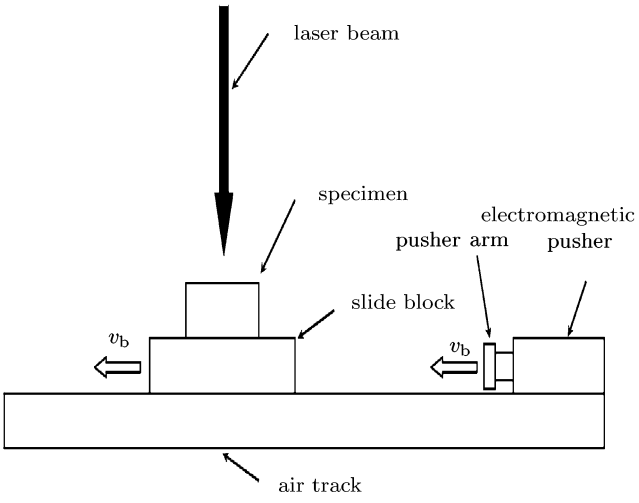


Fig.1. Schematic diagram of the surface remelting processing.

The present experiments were conducted on a 5kW continuous wave CO_2 laser (Rofin-Sinar 850). The laser beam was focused to a spot with the diameter of 0.5 mm and a continuous flow of He (10L/min) was blown onto the melting zone to prevent heavy oxidation during the laser treatment. The specimen was fixed on the slide block, which was floating on an air track. While the laser treatment was processed, the pusher arm provided an initial velocity, v_b, to the slide block. Then the slide block and the specimen moved straightly and steadily at v_b because there was no friction on the air track. The velocity of the block was between 6 mm/s and 1207 mm/s in the present experiment, which was measured by a light electric tachometer. Compared with the rotating disc method, we knew that the scanning velocity was obtained more smoothly and steadily by the present method and a straight laser trace was easier to analyse. The schematic diagram of the laser surface remelting processing is shown in Fig.1. After the laser treatment, a small quantity of white floccule could be observed on the surface of the samples, which resulted from the volatilization of Zinc under high temperature. In order to protect the operators from zinc poisoning, a gas extractor with a filter was placed near the laser beam during the laser treatment.

The specimens were cut along traverse and longitudinal directions of laser trace respectively. Then the samples were polished and etched with a solution of 100 mL of de-ionized water, 10g of Cr_2O_3 and $2-3$ drops of HCl. The microstructures of the samples were observed with a Hitachi S-570 scanning electron microscope (SEM) and optical microscope. In this paper, the angle θ was measured by employing a sampling method similar to the one adopted by Pan *et al.*[19]

3. Results

Figure 2 shows the SEM micrographs of the typical microstructures in the melting pool, where the black arrow indicates the direction of the laser beam velocity v_b. Featureless structures, which are the planar interface structure of the η phase growing under the ultra-high temperature gradient and low growth velocity condition, can be seen in the bottom of the melting pool (Fig.2(a)). In the laser melting pool, along with the increase of the distance from the bottom, the growth velocity increases and the temperature gradient decreases, as illustrated in Fig.3. In the upper section of the melting pool, due to a lower local

temperature gradient and a higher growth rate, the planar interface became unstable and lamellar structures appeared. With the increase of growth rate, the lamellar structure became more regular and the lamellar spacing decreased (Fig.2(b)). When the growth velocity reached 108 mm/s, lamellar structure transformed into a kind of structure with larger width and shallower grooves, which was identified as thin cellular structure in our previous paper,[20] as shown in Fig.2(c). As growth velocity increased to 210 mm/s, a cell-free structure was obtained.

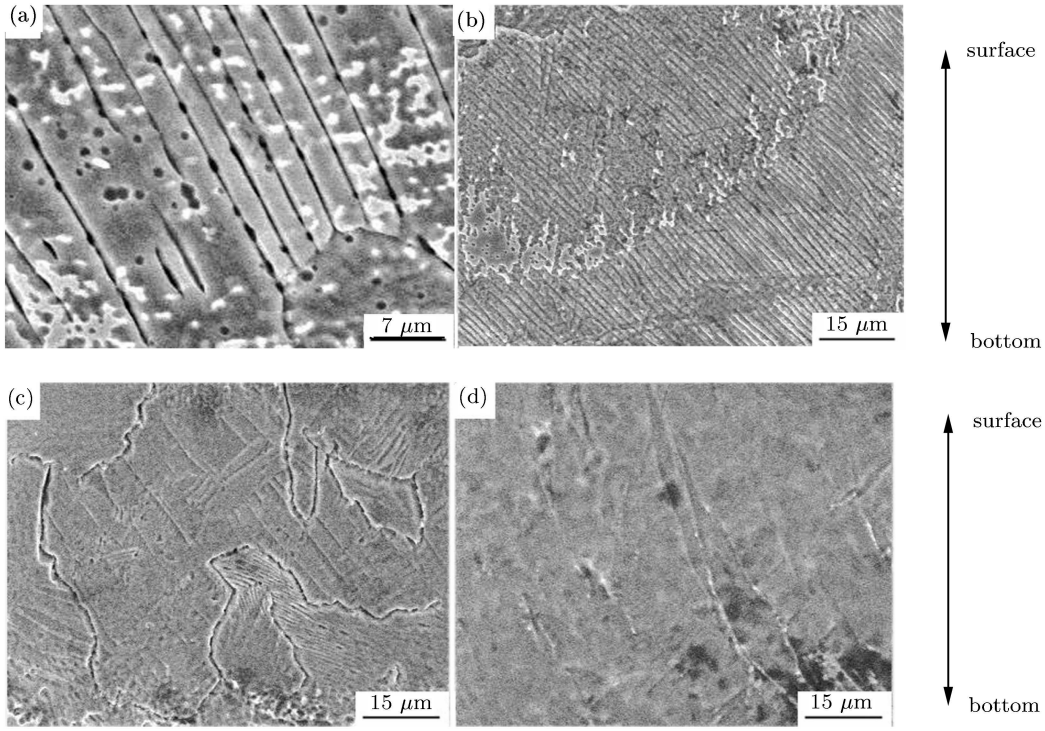


Fig.2. SEM micrographs showing the typical microstructures from longitudinal section of a laser resolidified Zn–2%Cu alloy under solidified velocities of 6.7 mm/s (a), 31.8 mm/s (b), 108.7 mm/s (c), and 210.0 mm/s (d).

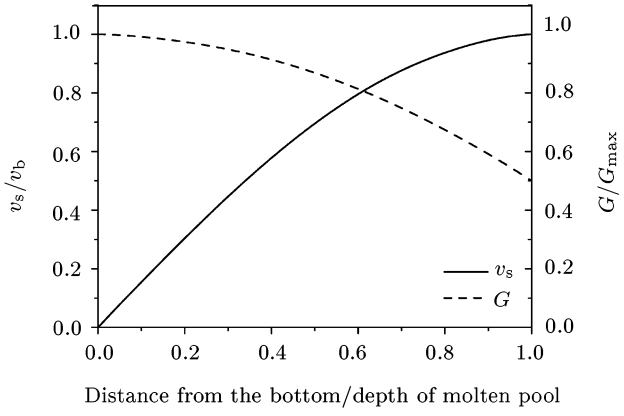


Fig.3. Schematic map of growth velocity and temperature gradient a various distances from the bottom of resolidified pool.

Finally, when the scanning velocity exceeded 652 mm/s, there were no visible microstructures throughout the whole molten pool (Fig.4). According to Ref.[20], the minimum spacing of the segregation structures, i.e. cells, dendrites or lamellar structures, is much larger than 0.8 μm and 0.24 μm, which are the minimum resolvable distance of Fig.4(a) and Fig.4(b), respectively. So it reveals that there are no segregation structures in the molten pool.

A JXA-733 electron probe microanalyser was employed to measure the composition of the cell-free structures in the melting pool at a scanning rate of 652 mm/s. The 10 measured points were randomly chosen in the cell-free structures. The results show that the Cu content in the cell-free structures is within

the range of 2.19–2.37 wt.%, which is slightly higher than the initial composition of the alloy. It can be attributed to the volatilization of Zinc under high temperature. Since there is no significant difference between the composition of the cell-free structures and the initial composition, further discussions will be based on the initial composition: 2.0 wt.%Cu.

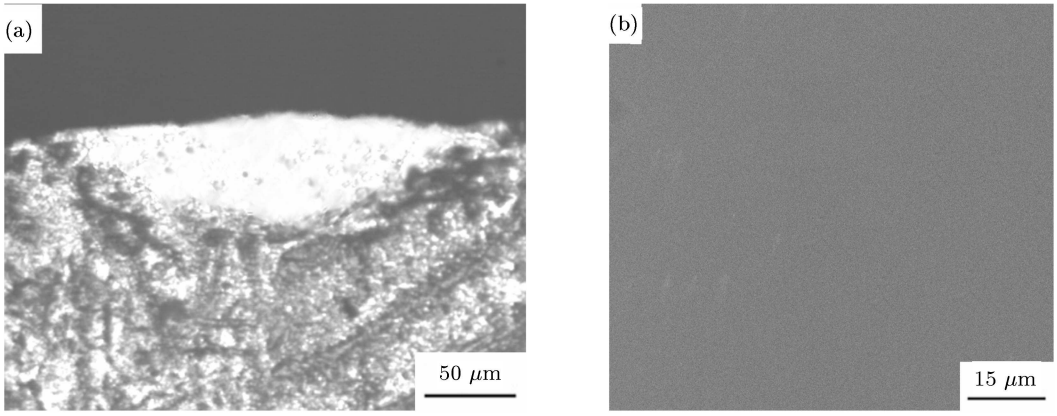


Fig.4. Fully cell-free microstructures morphology at a scanning velocity of 653 mm/s: (a) optical micrograph of the molten pool, (b) SEM micrograph of the microstructures in the molten poll.

4. Discussion

4.1. HVAS

According to the M–S interface stability theory,[2] the critical condition for the HVAS is given by

$$v_{\mathrm{ab}} = \frac{\Delta T_0 D_{\mathrm{L}}}{k_0 \Gamma}, \tag{1}$$

where k_0, Γ, D_{L} and ΔT_0 are the equilibrium partition coefficient, the Gibbs–Thomson coefficient, the solute diffusion coefficient and the freezing range of the alloy, respectively. For peritectic alloys, before determining v_{ab}, at first we should determine which phase is the leading phase under the local solidification condition. In our experiments, unidirectional solidification was achieved by using laser surface remelting technique and the nucleation process generally can be ignored during epitaxial growth. So it is reasonable to employ the maximum interface temperature criterion to predict the leading phase. According to the highest interface growth temperature criterion with the assumption of abundant nucleation condition, the phase with a higher interface temperature will be the leading phase during the unidirectional solidification.[21] So the interface response functions (IRF) of the planar interface of the two phases were calculated by using the following formulae given by Refs.[22–24]:

$$T_{\mathrm{p}}(v_{\mathrm{s}}) = T_{\mathrm{f}} + C_{\mathrm{l}}^{*} m_{\mathrm{v}} - (R_{\mathrm{g}} T_{\mathrm{f}} / \Delta S_{\mathrm{f}}) v_{\mathrm{s}} / v_0, \tag{2}$$

$$k_{\mathrm{v}} = \frac{k_{\mathrm{e}} + \alpha_0 v_{\mathrm{s}} / D_{\mathrm{i}}}{1 + \alpha_0 v_{\mathrm{s}} / D_{\mathrm{i}}}, \tag{3}$$

$$m_{\mathrm{v}} = \frac{1 - k_{\mathrm{v}}[1 - \ln(k_0 k_{\mathrm{v}})]}{1 - k_0} m, \tag{4}$$

where T_{f} is the melting temperature of the pure component, $C_{\mathrm{l}}^{*} = C_0 / k_{\mathrm{v}}$ is the concentration of the liquid at the interface, R_{g} is the gas constant, ΔS_{f} is the molar entropy of fusion, and v_0 is the limit of the crystalline growth velocity, whose upper limit equals to the velocity of sound. In equilibrium state, T_{p} corresponds to the solidus temperature of the initial composition C_0. The parameters used for the calculations were listed in Table 1.

The calculated results of the IRF for η and ε phases are shown in Fig.5. It can be seen that the η phase is the leading phase over the whole velocity range, so the theoretical critical velocities for the HVAS of Zn–2 wt.%Cu alloy can be determined. It equals to the critical velocity for the HVAS of the η phase, whose value is 48.2 mm/s. Attention must be given to what the experimentally determined critical velocity, 210 mm/s, for the HVAS (as shown in Fig.2(d)) is about 4.4 times of that predicted by M–S theory. In the previous papers, this kind of difference was often attributed to the effect of the possible impurity elements and the uncertainties of the thermophysical parameters.[13−16,28−30] In fact, the nonlinear instability of the planar interface is another important reason for it.

Table 1. Parameters for Zn–Cu diagram and thermophysical data of the phases involved solidification procedure

Parameters	Value	Reference
Melting point of Zn, T_{Zn}	692.73 K	[25]
Melting point of Cu, T_{Cu}	1358.02 K	[25]
Peritectic temperature, T_{p}	698.14 K	[25]
Liquid composition at peritectic reaction, C_{l}	1.7 wt.%	[25]
Composition in primary ε at peretectic reaction, C_{ε}	11.7 wt.%	[25]
Composition in peritectic η at peretectic reaction, C_{η}	2.75 wt.%	[25]
Liquidus slope of ε phase, m_{ε}	−17.1 K/wt.%Cu	[25]
Liquidus slope of η phase, m_{η}	−3.19 K/wt.%Cu	[25]
Equilibrium distribution coefficient of ε phase, k_{ε}	0.65	[25]
Equilibrium distribution coefficient of η phase (corrected), k_{η}	0.62	[25]
Diffusion coefficient in liquid, D_{L}	2.04×10^{-9} m^2/s	[26]
Diffusion coefficient in solid, D_{S}	1.59×10^{-12} m^2/s	[27]
Gibbs–Thompson coefficient, Γ	1.1×10^{-7} K·m	[26]

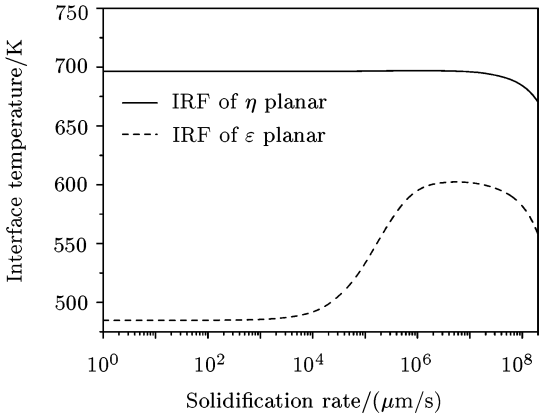


Fig.5. Calculated planar interface temperature varies with the solidified velocity for the two phases in solidification of Zn–2wt%Cu alloy.

In order to investigate the nonlinear instability of the planar interface and the dynamic bifurcation of the cellular–planar transition, an approach similar to the one adopted by Wu *et al*[31] has been employed. When a sinusoidal ripple perturbs the planar interface, the perturbed interface equation is

$$z = \phi(x,t) = \delta(t)\sin(\omega x), \tag{5}$$

where $\delta(t)$ is the amplitude of sinusoidal wave, $\omega = 2\pi\lambda$ is the frequency, and λ is the wavelength. The equations of the changed concentration and temperature field are

$$C(x,z,t) = C_0 + \frac{G_{\mathrm{C}}D}{v_{\mathrm{s}}}\Big[1-\exp\Big(-\frac{v_{\mathrm{s}}}{D}z\Big)\Big] + (b-G_{\mathrm{C}})\delta\sin(\omega x)\exp(-\omega^* z), \tag{6}$$

$$T'(x,z,t) = T_0 + \frac{G'D'_{\mathrm{th}}}{v_{\mathrm{s}}}\Big[1-\exp\Big(-\frac{v_{\mathrm{s}}}{D'_{\mathrm{th}}}z\Big)\Big] + (a'-G')\delta\sin(\omega x)\exp(-\omega'_{\mathrm{th}}z), \tag{7}$$

$$T(x,z,t) = T_0 + \frac{GD_{\mathrm{th}}}{v_{\mathrm{s}}}\Big[1-\exp\Big(-\frac{v_{\mathrm{s}}}{D_{\mathrm{th}}}z\Big)\Big] + (a-G)\delta\sin(\omega x)\exp(-\omega_{\mathrm{th}}z), \tag{8}$$

where $C(x,z,t)$ is the instantaneous concentration of solute in the liquid phase, C_0 is the liquid phase solute concentration at the unperturbed planar interface ($\delta = 0$), $T(x,z,t)$ and $T'(x,z,t)$ are the instantaneous temperature in the liquid phase and in the solid phase respectively, T_0 is the temperature of the unperturbed planar interface, G_{C} is the concentration gradient of solute in the liquid phase at the unperturbed planar interface, D is the diffusion coefficient of solute in the liquid phase, D'_{th} and D_{th} are the thermal diffusivity of the solid and liquid phase respectively, G' and G are the temperature gradient in the solid and liquid at the unperturbed planar interface, respectively, and

$$\omega^* = \frac{v_{\mathrm{s}}}{2D} + \Big[\Big(\frac{v_{\mathrm{s}}}{2D}\Big)^2 + \omega^2\Big]^{1/2}, \tag{9}$$

$$\omega'_{\mathrm{th}} = \frac{v_{\mathrm{s}}}{2D'_{\mathrm{th}}} - \Big[\Big(\frac{v_{\mathrm{s}}}{2D'_{\mathrm{th}}}\Big)^2 + \omega^2\Big]^{1/2}, \tag{10}$$

$$\omega_{\mathrm{th}} = \frac{v_{\mathrm{s}}}{2D_{\mathrm{th}}} - \Big[\Big(\frac{v_{\mathrm{s}}}{2D_{\mathrm{th}}}\Big)^2 + \omega^2\Big]^{1/2}. \tag{11}$$

After complex algebraic derivation, an implicit expression of the critical solidification velocity of the bifurcation point of the cellular–planar transition was obtained

$$F(v_{\mathrm{c}}) = m\frac{C_\infty(k-1)v_{\mathrm{c}}}{Dk} - (G_{\mathrm{T}} + \Gamma\omega^2)\Big(1 + \frac{v_{\mathrm{c}}k}{D\omega^* - v_{\mathrm{c}}}\Big) = 0. \tag{12}$$

This means that when $v_{\mathrm{s}} \le v_{\mathrm{c}}$ the interface will be cell mode and when $v_{\mathrm{s}} \ge v_{\mathrm{c}}$ it will be the planar interface.

Numerically solving Eq.(12), we obtained the critical velocity, and its value is 80.5 mm/s, which shows a much better agreement with the experimentally obtained critical velocity than that predicted by Eq.(1).

4.2. HGAS

In 1997, Ding *et al* performed a more rigorous nonequilibrium analysis of the M–S theory by combining analytic method with numerical model, and found a new stability phenomenon.[12] The critical condition of the M–S interface stability is as follows:

$$G' = A + \frac{A^2}{4k} - \frac{3A^{3/2}}{2}r - \frac{A^2(1-2k)}{4k}r^2, \tag{13}$$

$$A = \frac{v_s}{D\Delta T_0/k\Gamma}, \tag{14}$$

where r is the positive real root of the following equation:

$$r^3 + (2k-1)r - \frac{2k}{A^{1/2}} = 0 \tag{15}$$

and G' is the dimensionless temperature gradient defined as

$$G' = \frac{G}{\Delta T_0^2/kT}. \tag{16}$$

Equations (13)–(15) were numerically solved by Ding *et al* to obtain the maximum of G'. A regressive analysis of the calculated results was performed and the critical temperature gradient was obtained

$$G_a \cong \frac{\Delta T_0^2}{k_0\Gamma}(-0.0203k_0^3 + 0.0487k_0^2 - 0.0541k_0 + 0.0624), \quad 0 < k_0 < 1. \tag{17}$$

Equation (17) means that when $G \geq G_a$ the interface will be planar interface. It indicates that while the weighted mean temperature gradient G is above or equal to the critical value G_a, its stabilizing effect will entirely dominate the destabilizing effect of solute diffusion, so that the solidification interface becomes absolutely stable no matter how large the solidification velocity is, i.e. the interface stability is independent of the solidification velocity. Ding *et al* called this kind of absolute stability the high gradient absolute stability.

Substituting the parameters listed in Table 1 into Eq.(17) we get G_a of 1.65×10^6 K/m for the HGAS of the η phase. It is known that the temperature gradient in the melting pool increases with the scanning velocity.[19] It is found that, when the scanning rate reached 652 mm/s, cell-free structures were attained throughout the whole melting pool in our laser remelting experiments (Fig.4). Cell-free structure can result from both planar front growth and complete 'solute trapping'. However, according to Aziz's model,[32] the critical growth velocity for complete "solute trapping" is about 5 m/s, which is much higher than the growth velocity in the present melting pool (the maximum growth velocity has an order of magnitude of 1×10^{-1} m/s). So it is clear that these cell-free structures result from the planar front growth. Because the solidification rate varies continuously from zero to the maximum from the bottom to the top of the melting pool, it implies that the planar interface stability is independent of the solidification rate at a scanning rate of 652 mm/s. That is to say, these cell-free structures may be attributed to the result of the HGAS. However, before a conclusion can be drawn, the local temperature gradient in the laser melting pool must be determined. For the difficulties of direct measurement, a numerical enthalpy method model was applied in the calculation of temperature field. This model was established by Liu *et al*[18] and the results showed an excellent agreement with that of laser surface remelting experiments in Cu–Mn alloys.[33] The minimum temperature gradient in the laser molten pools of Zn–2 wt.% Cu alloy was calculated and shown in Fig.6.

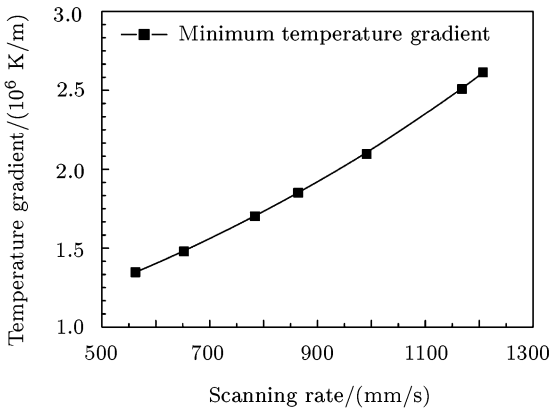


Fig.6. The minimum temperature gradient in the laser melting pool of Zn–2wt.%Cu alloy calculated by a numerical enthalpy method model.

It can be seen that the calculated minimum temperature gradient in the melting pool at a scanning rate of 652 mm/s is 1.48×10^6 K/m, which is very close to the critical temperature gradient for the HGAS of the η phase. So conclusion can be drawn that the HGAS was experimentally achieved in the laser surface remelting experiments on the Zn–2 wt.%Cu hypoperitectic alloy.

5. Conclusions

Laser surface remelting experiments of Zn–2 wt.%Cu peritectic alloy were performed on a 5kW CW CO_2 laser with various scanning velocities from 6 to 1207 mm/s. It was found that the critical solidification rate of the HVAS of Zn–2wt.%Cu hypoperitectic alloy is 210 mm/s. An implicit expression of the critical solidification rate for the cellular-planar transition was achieved by nonlinear stability analyses of the planar interface. The result showed a better agreement with the experimentally obtained critical velocity than that predicted by the M–S theory.

Cell-free structures were observed throughout the whole melting pool at a scanning rate of 652 mm/s. The minimum temperature gradient at this scanning rate, which was calculated by a numerical enthalpy method model, was very close to the HGAS of η phase. Conclusion can be drawn that the HGAS was experimentally achieved for the first time.

Acknowledgments

The authors would like to thank Miss Chen Q of Lanzhou University of Technology for her enthusiastic help.

References

[1] Mullins W W and Sekerka R F 1963 *J. Appl. Phys.* **34** 323
[2] Mullins W W and Sekerka R F 1964 *J. Appl. Phys.* **35** 444
[3] Trivedi R and Kurz W 1986 *Acta Metall. Mater.* **34** 1663
[4] Wollkind D J and Segel L A 1970 *Phil. Trans. Riy. Soc.* **268** 351
[5] Langer J S and Turski L A 1977 *Acta Metall.* **24** 1113
[6] Langer J S 1977 *Acta Metall.* **25** 1121
[7] Ungar L H and Brow R A 1984 *Phys. Rev.* B **29** 1367
[8] Schlitz L Z and Garimella S V 1984 *J. Appl. Phys.* **76** 4863
[9] Warren J A and Langer J S 1993 *Phys. Rev.* E **47** 2702
[10] Lin X, Li Tao, Wang L L, Su Y P and Huang W D 2004 *Acta Phys. Sin.* **53** 3971
[11] Huang W D, Lin X, Li Tao, Wang L L and Inatomi Y 2004 *Acta Phys. Sin.* **53** 3978
[12] Ding G L, Lin X, Huang W D and Zhou Y H 1997 *Materials Research Bulletin* **32** 669
[13] Boettinger W J, Shechtman D and Schaefer R J 1984 *Metall. Trans.* A **15** 55
[14] Gill S C and Kurz W 1993 *Mater. Sci. Eng.* A **173** 335
[15] Jones H 1991 *Mater. Sci. Eng.* A **133** 33
[16] Kurz W, Giovanola B and Trivedi R 1986 *Acta Metall.* **34** 823
[17] Gremaud M, Carrard M and Kurz W 1991 *Acta Metall. Mater.* **39** 1431
[18] Liu Z X, Huang W D and Yang S 2002 *Chin. Nonferrous Metals* **12** 458
[19] Pan Q Y, Huang W D, Lin X and Zhou Y H 1997 *J. Crystal Growth* **181** 109
[20] Su Y P, Lin X, Wang M, Xue L and Huang W D 2004 *Scripta Materialia* **51** 397
[21] Kubin L P and Estrin Y 1985 *Acta Metall.* **33** 397
[22] Trivedi R and Kurz W 1986 *Int. Mater. Rev.* **39** 823
[23] Boettinger W J and Coriell S R 1988 In: *NATO ASI Series E-No.* 114., edited by Sahm P R, Jones H and Adams C M (Dondrecht: Martinus Nijboff) p81
[24] Aziz M J and Boettinger W J 1994 *Acta Metall. Mater.* **42** 27
[25] Massalski T B 1986 *Binary Alloy Phase Diagram* (ASM: Metals Park) p16
[26] Liu H Y and Jones H 1992 *Acta Metall.* **40** 229
[27] Cahn R W and Haasen P 1996 *Physical Metallurgy* 4th edn (Amsterdam: North-Holland) p70
[28] Pan Q Y, Huang W D, Zhou Y H and Zhang G L 1998 *Mater. Res. Bull.* **33** 1621
[29] Yang S, Huang W D, Liu W J and Zhou Y H 2002 *Prog. Natural Sci.* **12** 684
[30] Yang S, Su Y P, Liu W J, Huang W D and Zhou Y H 2003 *Acta Phys. Sin.* **52** 81
[31] Wu J P, Hou A X, Huang D H, Bao Z Y, Gao Z N and Qu S S 2001 *Science in China* E **44** 484
[32] Aziz M J 1982 *J. Appl. Phys.* **53** 1158
[33] Yang S, Su Y P, Liu W J, Huang W D and Zhou Y H 2003 *J. Mater. Sci. Tech.* **19** 225